JOURNAL OF PROPULSION AND POWER
Vol. 19, No. 2, March–April 2003

Operational Sensitivities of an Integrated Scramjet Ignition/Fuel-Injection System

S. D. Gallimore,* L. S. Jacobsen,† W. F. O'Brien,‡ and J. A. Schetz§
Virginia Polytechnic Institute and State University, Blacksburg, Virginia 24061

Results are presented of experiments conducted in a supersonic wind tunnel on an integrated fuel-injection/ignition system, consisting of an aeroramp injector and a plasma-torch igniter. The main goals of the work were to determine how the lifting effect of the aeroramp affected the plasma jet, to ascertain how the injection of fuel through the aeroramp and the power supplied to the torch influenced the distributions of excited species downstream of the device, and to investigate any synergistic effects from the combination. The aeroramp was observed to have a strong lifting effect on the plasma jet, especially for injector momentum-flux ratios above 1.5. In addition, increases in the torch input power produced an exponential effect on the emission intensity of the excited-state species downstream of the plasma jet, but was not observed to influence the jet penetration height. The results demonstrate that the increased penetration of combustion enhancing radicals is largely a function of the fluidic mechanisms generated by the injector and, thus, aids the plasma torch in influencing the combustion kinetics farther into the freestream than would normally be possible.

Nomenclature

d_{eff}	=	effective injector jet diameter
d_j	=	diameter of torch orifice
M	=	Mach number
P_t	=	torch power
q	=	jet-to-freestream momentum-flux ratio
R^2	=	coefficient of variation
T_t	=	total temperature
x	=	streamwise coordinate
y	=	spanwise coordinate
z	=	vertical coordinate

Subscripts

inj	=	injector
t	=	plasma torch, stagnation value
∞	=	freestream

Introduction

THE overall goal of any aerospace propulsion engine is the efficient production of net positive thrust, and careful development of the engine combustor can create significant gains toward this purpose. With the added complexity of supersonic combustion, new difficulties arise with effective mixing, cooling requirements, and various losses to due to shock waves and wall friction. The development of a practical supersonic combustor design usually involves a tradeoff, one that balances the mixing and combustion characteristics with the necessary losses needed to achieve such conditions. One potential avenue of minimizing these losses lies in the careful integration of the fuel injection and ignition/flame-holding mechanisms. Successful ignition and flame holding by the use of a plasma torch in a supersonic crossflow has been well documented.[1–6] In addition, the enhanced mixing effects for fuel injected into a supersonic stream through multiple wall injectors arranged to produce streamwise vortices have been shown.[7–12] However, to date, few investigations have focused on the parallel development and integration of these devices. The present experiments were part of an extensive research program designed to investigate the integration of an aeroramp injector with a plasma torch and to search for possible synergistic effects of the combination. The goals of the experimental research presented here were to discover the extent to which the aeroramp provided a lifting effect on the plasma jet and to determine the trends associated with downstream radical emission through changes in the torch power and injector fuel flow rate.

The design and development of the aeroramp is reported by Jacobsen et al.,[10] however, the torch design is proprietary and cannot be released. Both methane and nitrogen were used as torch feedstocks to determine the effects of using excited hydrocarbon and nitrogen species on the intensity and distribution of fuel-plasma products. Injectants included both air, to investigate the lifting effect of the aeroramp, and ethylene, to determine how the injector fuel flow rate and torch power affected the distribution of excited species downstream of the device. Evaluations of a specific test condition were made by means of filtered photography, spectroscopic measurements, and total temperature sampling. When a variety of measurements in the local, near-downstream, and far-downstream regions is used, a better understanding of the overall dynamics of the device is gained. Filtered photography provided qualitative information on the emission intensity of the jet, spectroscopic methods were used to measure the distribution of excited-state species just downstream of the jet, and total temperature measurements supplied a far-downstream look at how the thermal energy from the torch mixed into the aeroramp plume.

Each of the measurement techniques demonstrated that the aeroramp had a profound effect on the penetration height of the plasma jet, particularly for injector momentum-flux ratios above 1.5. In contrast, the input power of the torch was observed to have almost no influence on the penetration height of the plasma jet, except for powers above 3000 W, where it demonstrated a slight increase in penetration height. Although the input power showed limited capability of influencing the penetration height of the jet, spectroscopic measurements downstream of the plasma jet showed that increasing

Received 8 October 2001; revision received 3 December 2002; accepted for publication 14 December 2002.

*Graduate Research Assistant, Mechanical Engineering Department; currently Aerospace Research Engineer, Hypersonic Air Breathing Propulsion Branch, NASA Langley Research Center, Mail Stop 168, Hampton, VA 23681-2199. Member AIAA.

†Graduate Research Assistant, Department of Aerospace and Ocean Engineering; currently NRA Research Associate, Aerospace Propulsion Office, Air Force Research Laboratories, 1950 Fifth Street, Room D224, Wright–Patterson AFB, OH 45433. Member AIAA.

‡J. Bernard Jones Professor, Mechanical Engineering Department. Associate Fellow AIAA.

§Fred Durham Chair, Department of Aerospace and Ocean Engineering. Fellow AIAA.

the torch power had an exponential effect on the emission intensity of plasma-fuel products. The results of each of these studies indicate that careful integration of these types of devices is essential to maximize the effectiveness of localized ignition aids such as a plasma torch. Simply altering the torch operating conditions is not always sufficient because torches do not have the fluidic penetration strength necessary for influencing the flowfield into the far freestream. As will be shown, the integrated device demonstrates a self-correcting feature, in that, as the momentum-flux ratio of the injector increases, thereby increasing the penetration height of fuel, the blockage and lifting effects on the plasma jet increase proportionally, allowing the radicals present within the jet to penetrate farther into the crossflow where the fuel is located.

Experimental Setup

Wind-Tunnel Facilities

The plasma torch was placed in the floor of an unheated wind tunnel as shown in Fig. 1a. The wind tunnel is a blowdown design with a full nozzle to accelerate the airflow to Mach 2.4, with a nozzle outlet area of 23 × 23 cm. The test duration was typically 8–10 s at a total pressure of 380 kPa, during which spectroscopic and total temperature measurements were collected. Spectroscopic measurements were made through a fused-silica window in line with the plasma torch exit, as shown in Fig. 1b. Temperature probing was performed at an x/d_j distance of 49.8 downstream of the torch using a three-pronged probe rake. The ratio of probe capture to recovery area is 5 to 1, resulting in a recovery factor of 0.95.

Plasma Torch

A low-power, uncooled plasma torch was used as the plasma source, with pure molybdenum anodes and 2% thoriated tungsten cathodes. The internal electrode and flow swirler geometries of the torch are similar to those reported in other studies.[4,13,14] The torch anode has a 1.59-mm-diam constrictor, with a length of 2.54 mm. Molybdenum anodes were used in experiments involving a methane feedstock for extended anode lifetimes, but copper was used for nitrogen feedstocks because active nitrogen was found to be extremely erosive to molybdenum. The cathode tip has a 20-deg half-angle cone and was adjusted to produce a 0.178-mm arc gap, defined as the linear distance between the start of the constrictor and circle of projection of the constrictor onto the cathode. In some cases when using nitrogen, the gap was increased to 0.267 mm to increase the energy added to the gas. Feedstock flow rates were set so that the torch chamber pressure was nominally 340 kPa (65 psia, $q_t \approx 1.20$) for each test. Torch powers ranged from 0.5 kW with a nitrogen feedstock up to 3.6 kW for methane, with a nominal current of 25 A.

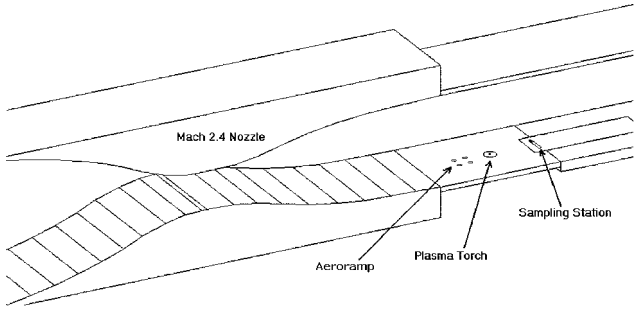

a) Schematic of injector, torch, and temperature sampling locations

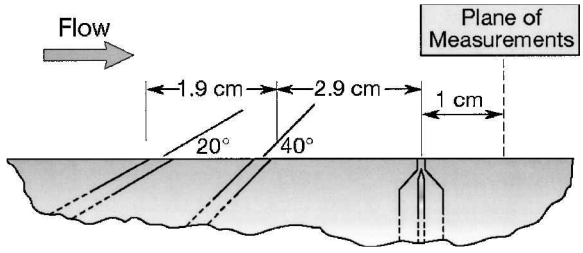

b) Spectral measurement plane

Fig. 1 Experimental setup of the aeroramp injector and plasma torch.

Charge-Coupled Device Spectrometer and Interference Filters

The charge-coupled device spectrometer system consists of three Ocean Optics S2000s, each with a spectral resolution of approximately 0.08 nm and a total spectral range from 196 to 730 nm. The three spectrometers, each with 25-μm interference slits and diffraction gratings with 1800 lines/mm, were used to achieve good spectral resolution while maintaining a spectral range encompassing the entire visible region. Stray light spilling over into other wavelengths is less than 0.10% throughout the dynamic range with a signal-to-noise ratio of 250:1 at full signal (≈62,500 full-well potential). The integration time for observing the plasma jet and downstream products was 125 ms. Photons emitted by the plasma jet entered a 1.0-mm-diam scope, fitted with a baffle to reduce the amount of reflected light entering the assembly (f number = 10.0). The scope was attached to a collimating lens, through which the photons were focused onto a 600-μm fiber optic cable. The cable was split into three 100-μm cables by means of a trifurcated splitter, each leg of which went to one of the three S2000s. All optical components, for example, cables, collimating lens, detector, etc., were selected for maximum transmission efficiency in the UV and visible wavelengths. A two-dimensional motorized traverse allowed movement of the point of observation during the experiments. Spectroscopic measurements of the plasma region were made at an angle of 10 deg off the perpendicular due to the location of the torch relative to the viewing window and spectroscopic apparatus.

Support of the spectroscopic measurements was made via the use of interference filters and a standard camera mounted perpendicularly to the tunnel flow. Each filter was selected based on the spectral wavelengths of excited species known to exist within the plasma jet. However, only the results of the studies conducted with the filter associated with CH^* emission at 431.4 nm are presented here because all filters produced qualitatively similar results. The filter used for CH^* transmission has a center wavelength of 431.4 nm, a half-bandwidth of 8.1 nm, and a maximum transmission efficiency of 46%.

Results and Discussion

Aeroramp Lifting Effect

Initial qualitative observations of the test section indicated that the addition of an upstream aeroramp injector had a strong effect on the penetration distance of the plasma jet, particularly for momentum-flux ratios in excess of 1.5. Figure 2 shows two black and white high-speed digital photographs of a nitrogen plasma jet (flow is from left

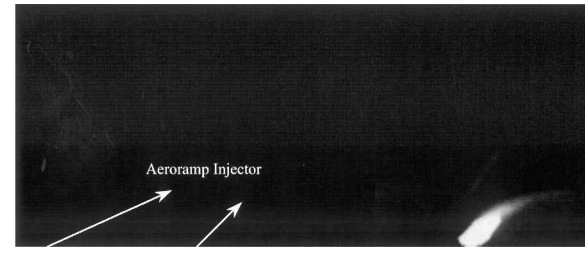

a) P_t = 900 W, q_t = 1.35, and q_{inj} = 0.00

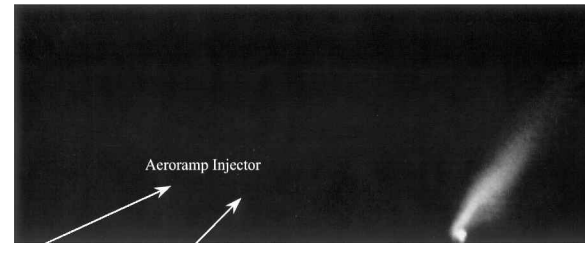

b) P_t = 770 W, q_t = 1.31, and q_{inj} = 3.67

Fig. 2 Lifting effect of an upstream aeroramp on a nitrogen plasma jet; scale 68 × 28 mm.

to right) with air fed through the upstream injector. Figure 2a shows that with no upstream injection the plasma jet exhibits a concentrated profile, with little penetration into the freestream. Increasing the mass flow rate of air through the injector allows for significantly greater penetration height, as shown in Fig. 2b for an injector momentum-flux ratio of 3.67. Experimental observations with a methane plasma jet produced similar trends and will be shown later. The increased penetration height is attributed to the combined effects of the protective barrier provided by the aeroramp and the lifting effect induced by the counter-rotating vortices. The magnitude to which each effect contributes to the propagation of excited-state species is uncertain, but methods of separating these effects would likely involve the use of devices in which the strength of the vortical motions could be varied without changing the Mach number of the downstream flowfield. Possibilities may involve a comparison between physical ramps with varying degrees of sweep, or aeroramps with varying toe-in angles.

Methane–Ethylene Experiments

Preliminary experiments with a methane feedstock and ethylene injectant focused on identifying the excited-state species within the torch exhaust. The spectrograph in Fig. 3 shows that only H^*, C^*, and C_2^* radiate with any appreciable intensity downstream of the torch exit, although peaks associated with CN^* and CH^* are observable under a reduced scale. The goal of the analysis was to identify an appropriate spectral line to measure under various operating conditions, thereby providing a means of comparison from one test case to another. Because of its intensity and extended lifetime compared to H^* and C^*, the emission of the C_2^* molecule (516.5 nm) was chosen as the measurement basis, particularly because no species associated with combustion, such as OH or H_2O, were present in sufficient concentration and excitation to produce strong band structures. The C_2 Swan bands shown in Fig. 3 are associated with hydrocarbon vapors passing through arcs with high-current density, as is the case here, in addition to being quite common in most rich premixed and nonpremixed flames. In the absence of combustion-indicative species, the study of the distribution of C_2^* provides a reasonable idea of trends associated with the design, such as the penetration height of excited-state species or the effect torch power has on the fuel-plasma kinetics.

When the spectrometer scope was traversed in the vertical direction, the distribution of C_2^* emission intensity was measured in a vertical plane 1 cm downstream of the torch exit. Figure 4 shows five intensity profiles for varying torch power with a constant injector momentum-flux ratio of 3.0. Each of the profiles exhibit spectral maxima between $d_j = 1.5$ and $d_j = 3.5$, with the spectral intensities dropping off linearly with distance above this region. As expected, the emission intensity at all measured locations increases with increasing power, but the torch input power was observed to have only a slight effect on the radical penetration height.

Plotting the maxima of the profiles from Fig. 4 in Fig. 5 demonstrates an exponential relationship between the torch input power and the intensity of the profile maxima. (Plots of the integral profile intensities produced similar trends.) As an example, comparison of

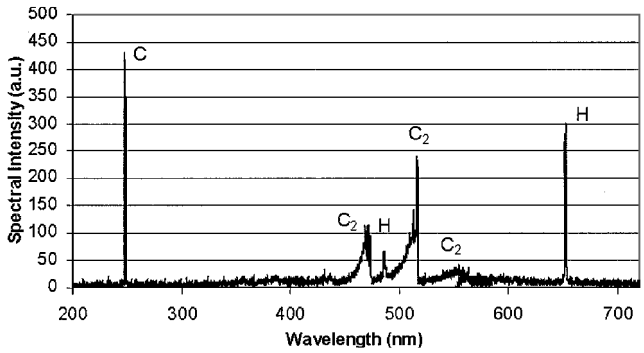

Fig. 3 Spectrograph of excited species generated via ethylene fuel and methane plasma interaction.

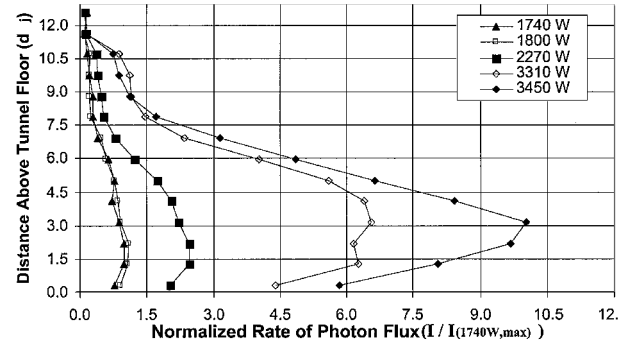

Fig. 4 Sensitivity of C_2^* profile intensity with increasing power using methane plasma, 1 cm downstream of torch exit, $q_t = 1.20$, and $q_{inj} = 3.00$.

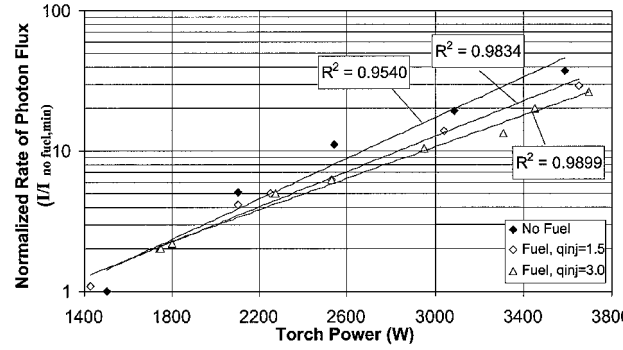

Fig. 5 Sensitivity of C_2^* profile maxima for varying injector momentum-flux ratios, $q_t = 1.20$, 1 cm downstream of torch exit.

the case for a $q_{inj} = 3.0$ demonstrates a 12-fold increase in the emission intensity of C_2^* from 1750 W to 3500 W, whereas at 2950 W the emission intensity increases by only a factor of 5. Although not presented here, measurements of the emission intensity of the plasma jet demonstrated only a linear increase with respect to the input power. When it is assumed that the jet intensity is representative of the concentration of excited-state species and can be well correlated to the concentration of ground-state species, the exponential increase in emission intensity downstream of the jet immediately points to effects governed by Arrhenius kinetics, which state that the reaction rate of a chemical mechanism is a function of the concentration of the species participating in that mechanism. This points back to the advantage of using a plasma-based ignition system, in that the localized population of species that participate in chain-initiation and chain-branching reactions is artificially increased, either through greater number densities within the jet, or through expansion of the jet volume. Both of these translate to greater intensities to an emission-sensitive device, but the effect is the same, that is, the ability of the jet to influence the chemical kinetics within the surrounding flowfield will increase. The effect of this is then what has been observed in Fig. 5, that is, the qualitative reactivity of the jet is being assessed through the measurement of the C_2^* emission intensity downstream of the jet.

Figure 5 also contains the results from two other test conditions; one with a momentum-flux ratio of 1.5 and another with no fuel fed through the injector. The immediate observation to be made from the chart is that an increase of the fuel flow rate through the injector causes a reduction in the emission intensity of the region downstream of the jet, where a comparison of the no-fuel to $q_{inj} = 3.0$ cases demonstrates almost a twofold reduction in the intensity of the C_2^* species downstream of the jet. The observation of lower intensities at higher fuel mass flow rates is a result of both the dilution of the plasma jet by ethylene and the higher thermal diffusivity of ethylene in comparison to air. The latter effect is directly related to the ability of ethylene to extract thermal energy more quickly from the jet without realizing a large gain in stored energy, in essence limiting the ability of the jet to dissociate the fuel. However, the point to be made is not that an increase of the fuel flow rate through the injector diminishes the effect of the torch, which would be a misleading

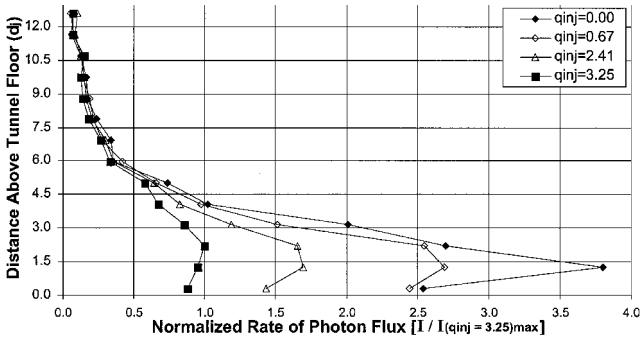

Fig. 6 Sensitivity of C_2^* profile intensity for various injector momentum-flux ratios using methane plasma, $P_t = 2500$ W, $q_t = 1.20$, 1 cm downstream of torch exit.

conclusion given the cold freestream conditions. Rather, the demonstration of sustained plasma-jet interaction with the injectant, even at high momentum-flux ratios, indicates that the placement of the plasma torch relative to the injector is such that these interactions are sustained over a wide range of injector operating conditions. An increase in the emission intensity at higher fuel flow rates would actually identify a condition where the quantity of fuel interacting with the jet has decreased, an undesirable effect. To further illustrate the point, it might be possible at high-momentum-flux ratios to inject a large fraction of the fuel into a region where the plasma jet has little influence. However, as will be shown shortly, high momentum-flux ratios also create large flow blockage and stronger vortices, both of which are conducive to allowing greater penetration of the plasma-jet radicals and, thus, increasing the ability of the jet to interact with the injectant, a self-correcting phenomenon.

In addition to the results of Fig. 5, which illustrate that the introduction of fuel to the plasma jet is maintained at high-momentum-flux ratios, Fig. 6 shows that a substantial lifting effect is present. Increasing the injector momentum-flux ratio from 0.67 to 3.25 almost doubles the penetration height of the profile maxima from 2 to just under 4 mm. Although the effect appears negligible, the importance lies in that the observed effect was completely unattainable by the use of excessively high-input torch powers. Furthermore, this occurs at a position very close to the plasma-torch exit, for which the benefits of penetration locally will extend to the far downstream.

Filtered photographic measurements support the observations made in Figs. 4–6. An interference filter associated with the emission of CH^* was used for these studies and allowed for a straightforward method of identifying regions containing high concentrations of excited-state species. Five photographs, of CH^* emission are presented in Fig. 7 for powers ranging from 1430 to 3650 W. Expectedly, as the power supplied to the torch increases, both the intensity and volume of the jet increase, but the added power does not seem to affect appreciably the penetration height. In contrast, the penetration height of the plasma jet was much more heavily influenced by the mass flow rate of fuel fed through the injector, as demonstrated in Fig. 8. In this case, a wide range of injector momentum-flux ratios was investigated to determine more accurately when the localized lifting effect of the aeroramp becomes significant. As shown in Fig. 8, aeroramp injector momentum flux ratios below 1.25 produce no noticeable effect on the shape or penetration height of the plasma jet. However, Fig. 8d clearly shows increased penetration for an injector momentum-flux ratio of 1.62. Not only is the lifting effect observable in the outer boundaries of the jet, but the core seems to be appreciably affected as well, particularly for momentum-flux ratios above 1.62. The specific momentum-flux ratio where the lifting effect becomes appreciable is less well defined, but for clarity in future discussions it will be assumed to be approximately 1.5. This value will also change for different flowfield conditions, and so this aspect of the results should be noted as well.

Total temperature measurements allowed the evaluation of how the thermal energy contained within the plasma jet mixed into the aeroramp plumes. A two-dimensional total temperature ratio profile for a torch power of 2000 W and an injector momentum-flux ratio of 1.5 is shown in Fig. 9. The symmetric structure of the total temperature in Fig. 9 indicates that the thermal energy imparted by the plasma jet is evenly distributed into both sides of the injector plume. In addition, the mushroomlike appearance of the plume indicates, as with the CH^* photographs, that the thermal energy contained within the jet is lifted off the floor of the tunnel and into the crossflow. Although not shown here, experiments with only a plasma torch produced profiles with higher total temperature ratios (due to the absence of the dilution and thermal diffusivity effects discussed earlier), but had significantly lower penetration, with the value of $(T_t/T_{t,\infty})_{\max}$ located at approximately $Z/d_{\text{eff}} = 0.75$. Thus, the results presented here show that the penetration has increased more than twofold and that mixing of the plasma jet exhaust into the freestream has improved due to the addition of an upstream aeroramp. Measurements with a nitrogen plasma jet showed that the penetration height was independent of the feedstock gas for equivalent flow rates and powers. Again, this demonstrates that the penetration of the thermal energy, that is, excited-state species, is greatly assisted by the upstream aeroramp and is only a weak function of the torch operating conditions.

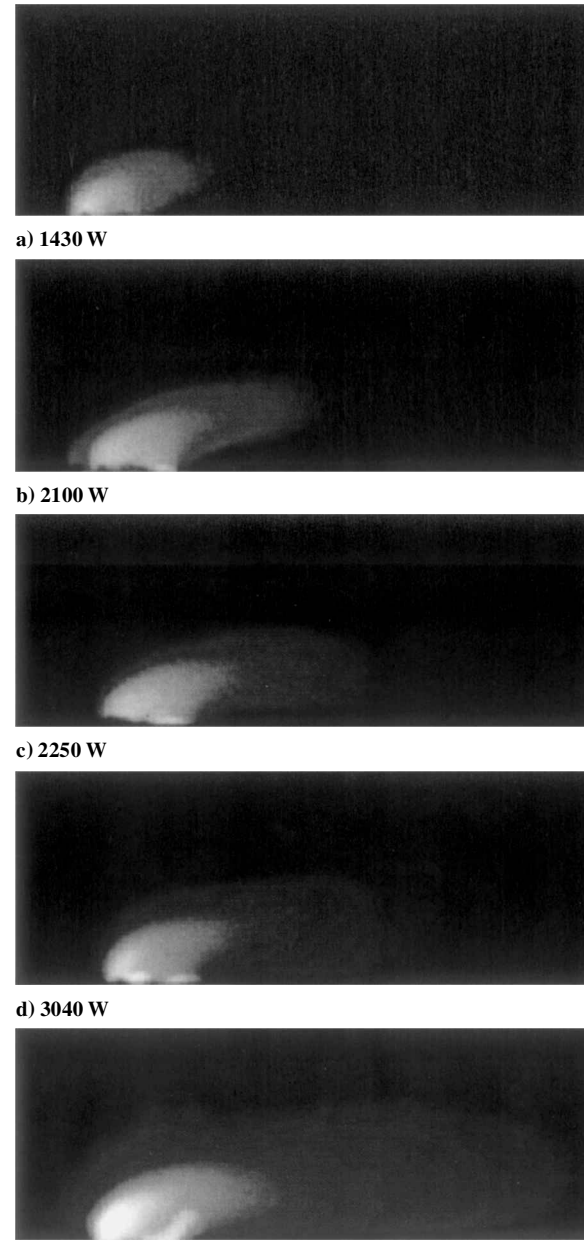

Fig. 7 CH Profile variations with increasing power, $q_t = 1.20$, $q_{\text{inj}} = 1.50$, experiment time: 8 ms, with scale 17 × 6 mm.

a) $q_{inj} = 0.00$

b) $q_{inj} = 0.85$

c) $q_{inj} = 1.25$

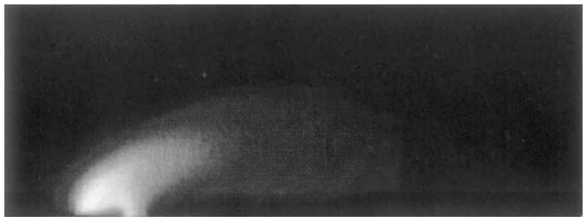

d) $q_{inj} = 1.62$

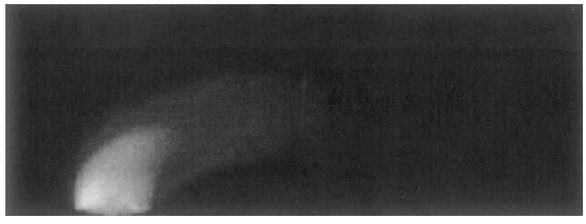

e) $q_{inj} = 2.41$

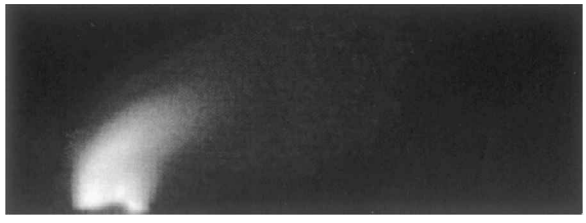

f) $q_{inj} = 3.06$

Fig. 8 CH profile variations with increasing injector mass flow rate; $P_t = 2500$ W, $q_t = 1.20$, experiment time 8 ms, with scale 17 × 6 mm.

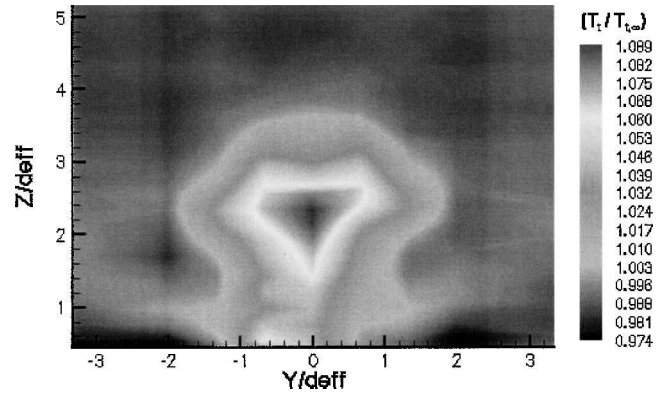

Fig. 9 Two-dimensional temperature profile of ethylene–methane experiments at 2000 W, $P_t = 2000$ W, $q_t = 1.20$, and $q_{inj} = 1.50$.

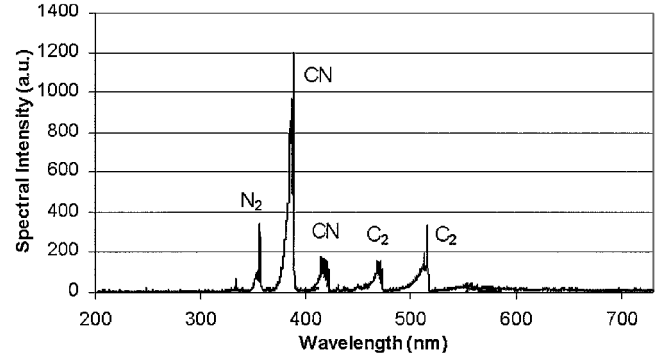

Fig. 10 Spectrograph of excited species generated via ethylene fuel and nitrogen plasma interaction.

Nitrogen–Ethylene Experiments

As with the methane–ethylene experiments, the first step in the nitrogen–ethylene studies was to ascertain the type of excited-state species present within the torch exhaust. A typical spectrograph taken of the plasma jet exhaust is shown in Fig. 10. The spectrograph indicates that little, if any, combustion effects are taking place in this region through the absence of combustion intermediates or products such as OH, CH, or H_2O. More important though, the presence of C_2^* and CN^*, both products of a hydrocarbon vapor being introduced to active nitrogen, clearly indicates plasma/fuel interaction. This is in contrast to the methane experiments, where it was impossible to identify the magnitude to which each hydrocarbon source contributed to the overall intensity of the plume. Atomic species, such as H^* and C^* will be shown to exist only near the torch exit where the energy density is highest and so are absent here. For the experiments involving a nitrogen feedstock and ethylene injectant, the intensity of CN^* emission was chosen as the measurement basis because the CN^* line at 388.3 nm is stronger here than the C_2^* line at 516.5 nm, which was the basis of comparison in the methane-based experiments.

Because the input power and injectant mass flow rate characteristics have been demonstrated already and showed similar trends in the nitrogen-based studies, only the studies associated with variations of the arc gap will be shown here. The motivation behind the investigation is that the relatively low specific heat and high thermal diffusivity of nitrogen, when compared to methane and longer-chain hydrocarbons, makes it challenging to extract a large amount of energy from the arc, particularly for the short arc lengths used with hydrocarbon operation. Experiments with arc gaps of 0.178 and 0.267 mm were conducted to determine how the arc length influenced the emission intensity of the fuel/plasma products. The results of the spectroscopic surveys are shown in Fig. 11. For a given torch input power, the CN^* profile intensities are much higher for the longer arc gap than for the shorter arc gap, which is indicative of a higher rate of energy transmission to the gas by the arc. In addition, like with the experiments involving the methane feedstock, the penetration heights of the CN^* profile maxima demonstrate some slight dependence on torch input power, but are totally independent of the length of the arc gap. Again, this continues to solidify the point that to increase the penetration of combustion enhancing species, alterations to the torch operating conditions are insufficient; another fluidic or physical device is required.

Although the penetration height of excited-state species exhibited no dependence on the arc length, the maxima of the profiles presented in Fig. 11 do. As shown in Fig. 12, an increase of the

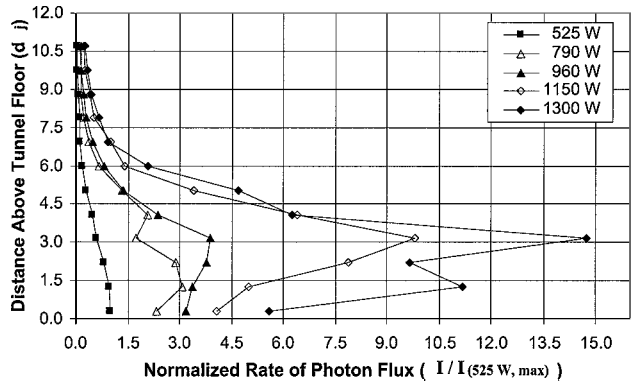

a) Arc gap of 0.178 mm

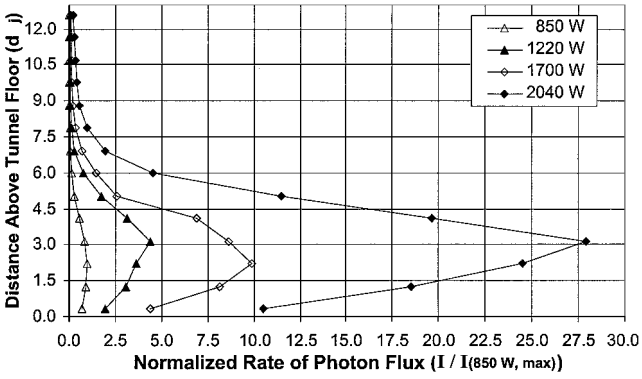

b) Arc gap of 0.267 mm

Fig. 11 Sensitivity of the CN* profile intensity vs arc gap for nitrogen plasma, 1 cm downstream of torch exit, $q_t = 1.2$, $q_{inj} = 1.5$, with CN line at 388.3 nm.

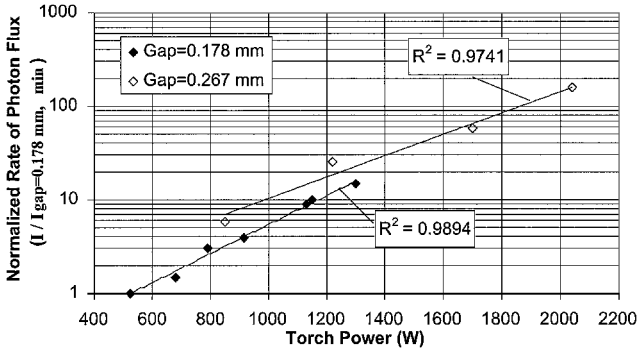

Fig. 12 Sensitivity of CN* profile maxima vs arc gap, $q_t = 1.2$, $q_{inj} = 1.5$, 1 cm downstream of torch, with CN line at 388.3 nm.

arc gap serves to increase the emission intensity of excited-state species for a given power, a result of the longer path of energy transfer. This would suggest then that larger arc gaps are preferred until the constrictor thermal entry length is reached for the given current, at which point any further increases in power will result in a greater radiation loss to the electrodes as opposed to further dissociation of the gas.[15] Furthermore, because CN* is produced only through the chemical and thermal interaction of the ethylene injectant and nitrogen plasma jet, the trends observed in Fig. 12 can now convincingly be correlated to the amount of fuel dissociated by the torch. Unlike with the methane-based experiments, where the contributions of dissociated injectant and feedstock to the emission intensity of the torch plume could not be separated, here it is quite evident that the emission intensity is directly related to the amount of energy exchange between the fuel and plasma, either through direct dissociated or various chemical reactions. As stated earlier, the emission intensity is a function of input power, indicating that increasing the power supplied to the torch creates an exponential return in the production of excited-state species and ultimately in the ignition and flame-holding potential of the integrated device.

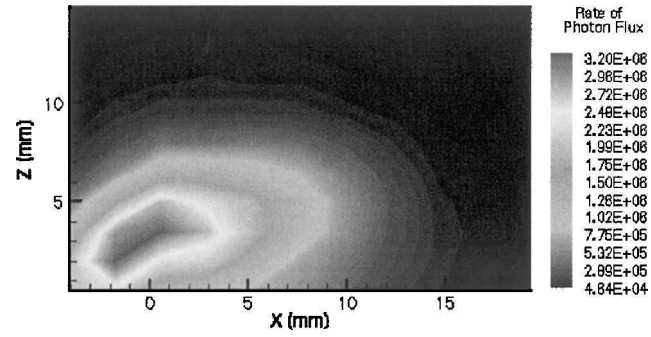

a) N_2 Profile (357.7 nm)

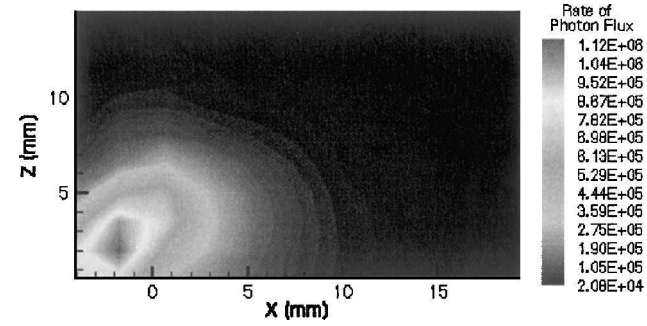

b) C Profile (247.8 nm)

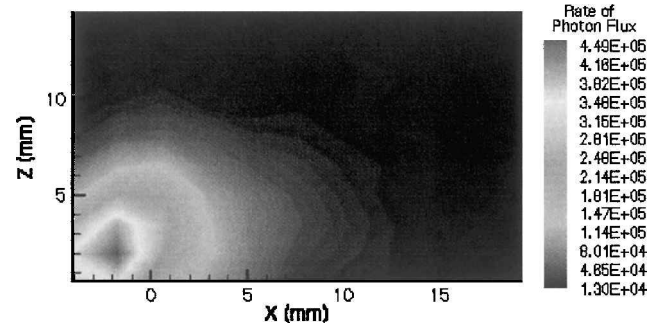

c) H Profile (656.3 nm)

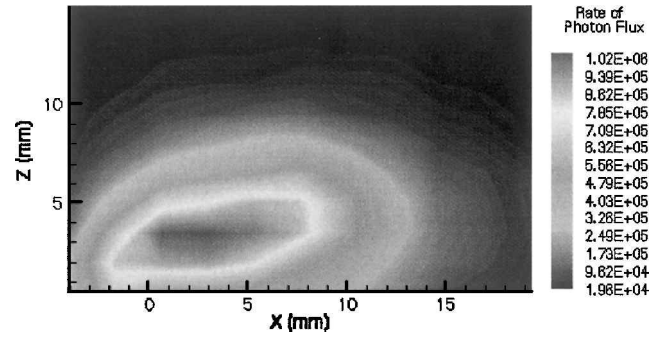

d) C_2 Profile (516.5 nm)

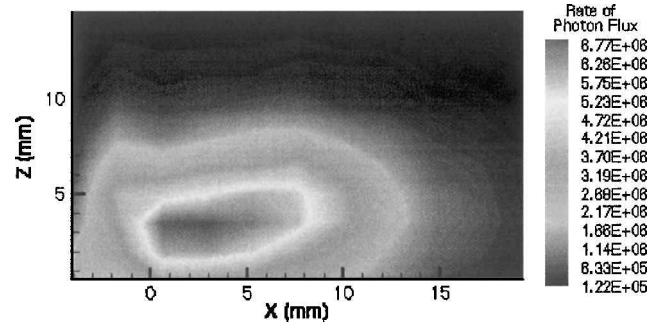

e) CN Profile (388.3 nm)

Fig. 13 Radical profiles near torch exit, $P_t = 2040$ W, $q_t = 1.24$, $q_{inj} = 1.50$, with arc gap of 0.267 mm.

Spectral data at other locations were taken to improve the understanding of the distributions of excited species within and around the jet and were used to construct intensity profiles near the torch exit as shown in Fig. 13. (Torch exit is located at $x = 0$ mm.) Figure 13a shows a profile for excited N_2 and provides a good indication of the plasma-jet boundary, as opposed to its region of influence marked by hydrocarbon fragments and CN^*. The profiles of atomic carbon and hydrogen in Figs. 13b and 13c indicate the most intense regions of interaction, where, through intense thermal and chemical interaction with the plasma jet, some of the fuel molecules have been dissociated into their atomic components. The maxima of atomic carbon and hydrogen occur just upstream of the plasma torch exit in a subsonic separation region. These atomic species reach the ground state or recombine before they propagate more than 6 or 7 mm from the plasma-torch exit, which clearly illustrates the need for careful integration of the plasma torch into a fuel-injection system to maximize the likelihood that short-lived combustion enhancing species react with fuel. The C_2^* and CN^* profiles in Figs. 13d and 13e are qualitatively similar in shape and identify the localized region in which the plasma jet most readily influences the freestream. The C_2^* and CN^* molecules exhibit maxima directly above the torch exit and persist approximately the same distance downstream before reaching the ground state or recombining with other species. Evidence of excited CN^* and C_2^* is present in front of the plasma jet as well, formed in the recirculation region between the jet centerline and bow shock.

Conclusions

The experiments presented here were part of an extensive research program designed to investigate the integration of an aeroramp injector and plasma torch and to discover if any synergistic effects exist as a result of the integration. The goals of the research were to determine the extent to which the aeroramp injector assists the propagation of radicals contained within the plasma jet by means of the counter-rotating vortices and blockage effects. Variations in the fuel flow rate through the injector and the power of the torch were made to assess how various operating conditions changed the performance of the design. Spectral measurements, filtered photography, and total temperature sampling were used to provide a full-picture view of the local, near-downstream, and far-downstream phenomena associated with the design. The main observations made from the research are as follows.

1) The aeroramp injector significantly increases the penetration height of excited-state species contained within the plasma jet, particularly for injector momentum-flux ratios of approximately 1.5 and above. An injector momentum-flux ratio of 3.06 produced approximately twofold greater radical penetration than for conditions with no fuel fed through the injector.

2) Comparison of the total temperature measurements for conditions with and without the use of an aeroramp injector indicates an increase of approximately 100–150% in the penetration height of the plume core for a momentum-flux ratio of 1.5 at a downstream location of $x/d_j = 49.8$.

3) Increasing the torch power was observed to cause an exponential increase in the emission intensity of downstream products, for both methane and nitrogen feedstocks, indicative of greater plasma jet reactivity and influence on the surrounding flowfield.

4) Total temperature measurements showed that the thermal energy contained within the plasma jet was distributed symmetrically into the injector plume produced by the aeroramp.

Based on the observations presented, the integrated injection/ignition design appears to have promising mixing, penetration, and ignition potential for supersonic combustion applications. The next step in the research plan is to conduct experiments in a high-speed combustion facility to quantify better the performance characteristics of the integrated design. The tests will specifically target the investigation of combustion efficiency for various operating conditions and identifying the flame-holding limits of the design.

Acknowledgments

The plasma-igniter/aeroramp integration was initially developed under subcontract to, and in cooperation with, Phoenix Solutions Company under a U.S. Air Force Small Business Innovation Research Phase II plasma igniter program with U.S. Air Force Research Laboratory.

References

[1]Kato, R., and Kimura, I., "Numerical Simulation of Flame-Stabilization and Combustion Promotion by Plasma Jets in Supersonic Air Streams," *Twenty-Sixth International Symposium on Combustion*, Combustion Inst., Pittsburgh, PA, Vol. 26, 1996, pp. 2941–2947.

[2]Kimura, I., Aoki, H., and Kato, M., "The Use of a Plasma Jet for Flame Stabilization and Promotion of Combustion in Supersonic Air Flows," *Combustion and Flame*, Vol. 42, 1981, pp. 297–305.

[3]Northam, G. B., McClinton, C. R., Wagner, T. C., and O'Brien, W. F., "Development and Evaluation of a Plasma Jet Flameholder for Scramjets," AIAA Paper 84-1408, June 1984.

[4]Wagner, T. C., O'Brien, W. F., Northam, G. B., and Eggers, J. M., "Plasma Torch Igniter for Scramjets," *Journal of Propulsion and Power*, Vol. 5, No. 5, 1989, pp. 548–554.

[5]Takita, K., Uemoto, T., Sato, T., Ju, Y., Masuya, G., and Ohwaki, K., "Ignition Characteristics of Plasma Torch for Hydrogen Jet in an Airstream," *Journal of Propulsion and Power*, Vol. 16, No. 2, 2000, pp. 227–233.

[6]Shuzenji, K., Kato, R., and Tachibana, T., "Ignition Characteristics of Arc Discharges Exposed to Supersonic Airflows," AIAA Paper 2000-0617, Jan. 2000.

[7]Sato, Y., Sayama, M., Katsura, O., Masuya, G., Komuro, T., Kudou, K., Murakami, A., Tani, K., Wakamatsu, Y., Kanda, T., and Chinzei, N., "Effectiveness of Plasma Torches for Ignition and Flameholding in Scramjet," *Journal of Propulsion and Power*, Vol. 8, No. 4, 1992, pp. 883–889.

[8]Schetz, J. A., Cox-Stouffer, S., and Fuller, R., "Integrated CFD and Experimental Studies of Complex Injectors in Supersonic Flows," AIAA Paper 98-2780, June 1998.

[9]Jacobsen, L., Schetz, J., Gallimore, S., and O'Brien, W., "Mixing Enhancement by Jet Swirl in a Multiport Injector Array in Supersonic Flow," *3rd ASME/JSME Joint Fluids Engineering Conference*, Rept. FEDSM99-7248, San Francisco, CA, July 1999.

[10]Jacobsen, L., Schetz, J., Gallimore, S., and O'Brien, W., "An Improved Aerodynamic Ramp Injector in Supersonic Flow," AIAA Paper 2001-0518, Jan. 2001.

[11]Fuller, R. P., Wu, P. K., Nejad, A. S., and Schetz, J. A., "Fuel–Vortex Interactions for Enhanced Mixing in Supersonic Flow," AIAA Paper 96-2661, July 1996.

[12]Cox, S. K., Fuller, R. P., Schetz, J. A., and Walters, R. W., "Vortical Interactions Generated by an Injector Array to Enhance Mixing in Supersonic Flow," AIAA Paper 94-0708, Jan. 1994.

[13]Barbi, E., Mahan, J. R., O'Brien, W. F., and Wagner, T. C., "Operating Characteristics of a Hydrogen–Argon Plasma Torch for Supersonic Combustion Applications," *Journal of Propulsion and Power*, Vol. 5, No. 2, 1989, pp. 129–133.

[14]Stouffer, S., "Development and Operating Characteristics of an Improved Plasma Torch For Supersonic Combustion Applications," Masters Thesis, Mechanical Engineering Dept., Virginia Polytechnic Inst. and State Univ., Blacksburg, VA, July 1989.

[15]Mahan, J. R., "An Experimental Study of the Effects of Local Fluid Constriction on the Confined Discharge Plasma Generator," Ph.D. Dissertation, Mechanical Engineering Dept., Univ. of Kentucky, Lexington, KY, Dec. 1970.